The Nature of Rhodopsin-Triggered Photocurrents in *Chlamydomonas*. I. Kinetics and Influence of Divalent Ions

Eva-Maria Holland,* Franz-Josef Braun,* Christina Nonnengässer,‡ Hartmann Harz,‡ and Peter Hegemann*‡

*Institut für Biochemie I, 93040 Regensburg, and ‡Max-Planck-Institut für Biochemie, 82152 Martinsried, Germany

ABSTRACT In the green alga *Chlamydomonas* chlamyrhodopsin fulfills its role as a light sensor by absorbing light and activating photoreceptor channels within the eyespot area. At intense light stimuli, the photoreceptor (P) current triggers a fast and a slow flagellar current that finally leads to backward swimming (stop response). Here we report about probing the photoreceptor current directly at the eyespot. This allows the detection of the whole P current with a size of above 50 pA. The P current appears with a delay of less than 50 μs, suggesting that rhodopsin and the P channel are closely coupled or form one ion channel complex. The Ca^{2+} dependence of the P current has been demonstrated with the established suction technique in a capacitive mode. The P current shows the maximum amplitude at only 300 nM Ca^{2+}, and it gradually declines at higher Ca^{2+}. In addition to Ca^{2+}, the photoreceptor and the fast flagellar current can be carried by Sr^{2+} and Ba^{2+}. Mg^{2+} is conducted less efficiently and at high concentrations blocks the photoreceptor channel. A motion analysis of the cells shows that only Ca^{2+} and Sr^{2+} can induce physiological stop responses, whereas the large Ba^{2+} currents cause abnormal long-lasting cell spiraling.

INTRODUCTION

Most motile unicellular algae can orient themselves in their light environment. They swim toward or away from a light source, and when the intensity of the light drastically changes they perform distinct directional changes or stop responses. In *Chlamydomonas*, these behavioral responses are mediated by chlamyrhodopsin, which serves as the sensory photoreceptor (Foster et al., 1984; Uhl and Hegemann, 1990). Its all-*trans* retinal chromophore (Beckmann and Hegemann, 1991; Hegemann et al., 1991; Lawson et al., 1991; Takahashi et al., 1991) bears strong functional relationship to bacterial rhodopsins (Zacks et al., 1993). The opsin sequence is not homologous to bacterial opsins; rather it shows significant relation to animal rhodopsins, especially to those from invertebrates (Deininger et al., 1995). The opsin contains many charged or polar residues, and only four transmembrane segments can be identified. This suggests that the signal transduction mechanism differs from that initiated by all other members of the rhodopsin superfamily. Electrical measurements demonstrated that a very rapid signal transduction from the rhodopsin to the flagella takes place via a sequence of electrical processes in *Chlamydomonas* and its relative *Haematococcus* (Sineshchekov et al., 1990; Harz et al., 1992), whereas rhodopsin-mediated signaling, which is based on biochemical ampli-

fication, occurs on a much slower time scale in animals as well as in *Halobacteria*. Strictly speaking, electrical signaling in *Chlamydomonas* only can explain transient photophobic responses, whereas direction changes and phototaxis still remain to be understood.

Light-triggered electrical events in *Chlamydomonas* have been difficult to analyze in detail over the years and still pose many problems and unanswered questions for scientists. Intracellular recording has been precluded by the small size of the alga and especially by the small cytoplasmic volume. Upon insertion of micropipettes the membrane potential collapses and flagellar beating can only be maintained in the presence of Mg^{2+} and ATP (noteworthy experiments were presented by Nichols and Rickmanspoel, 1978). Patch-clamp experiments with $G\Omega$ cell-to-pipette seals were carried out, but no consistent results have been obtained so far because of cell surface impurities, even in cell wall-less mutants (Sullivan and Foster, 1987; Braun and Hegemann, unpublished observations). Currently, only a suction pipette technique can be successfully applied to *Haematococcus* (Litvin et al., 1978) and to *Chlamydomonas* cell-wall-deficient or autolysin-treated cells (Harz and Hegemann, 1991).

When a suction pipette is applied to a cell-wall-deficient *Chlamydomonas* cell and the cell is stimulated by short but intensive flashes, one can observe a pattern of three photocurrents. The first transient current is localized in the eyespot; this has been termed the photoreceptor current (P). To understand the signal transduction chain, it is necessary to know how the chlamyrhodopsin is coupled to the photoreceptor channel and whether it is part of the channel complex (Deininger et al., 1995). Therefore measurements with high time resolution are required. The second transient current is localized in the flagella; this has been named the fast flagellar current (F_F). The flagellar current is distributed along the whole flagellar length (Beck and Uhl, 1994). The

third current is a slow flagellar current (F_S), with very small amplitude under physiological conditions. At present its exact flagellar distribution is unknown. Flagellar currents only appear at high flash energies ($>1 \times 10^{18}$ photons m^{-2}, green light) as all-or-none events. Because the P current integral has to overstep a critical level before F currents appear, it has been suggested that the F currents are voltage-dependent processes and serve as the trigger for photophobic responses (stop responses) (Harz et al., 1992). Although the slow flagellar current (F_S) has not been characterized in any detail, it has been held responsible for maintaining the cells in the backward swimming mode for an extended period (Harz et al., 1992). The cellular structures to which the Ca^{2+} finally binds have not been clearly identified, although evidence suggests that calmodulin and a 75-kDa flagellar protein could be the primary Ca^{2+} acceptors (Witman, 1994). The flagellar events occuring at low light levels where no flagellar currents are detected are still unknown.

In the present study, we concentrate further on the high-light-intensity responses, especially on their kinetics and ionic nature and the detection of regulatory processes.

MATERIALS AND METHODS

All experiments were carried out with the cell-wall-deficient mutant CW2.

Nonspecified reagents were from Sigma and of analytical grade.

Cells were grown on agar plates of high-salt acetate medium (HSA) with 250 mM sorbitol, and cells were differentiated into gametes in the absence of sorbitol in nitrogen-deficient minimal medium (NMM) at 4 W m^{-2} white light under conditions described in detail by Harz et al. (1992). The most phototactically active cells were selected by performing three rounds of photoselection in the measuring buffer. After further incubation in light for 1 h and dark adaptation for at least another hour, cells were used for electrical measurements.

In most experiments a NMG$^+$/K$^+$ buffer was used (5 mM HEPES, 9 mM HCl, 1 mM KCl, 200 μM K-BAPTA, L-BAPTA (1,2-bis(2-amino-phenoxy)ethane-N,N,N',N'-tetraacetic acid, tetrapotassium salt) adjusted with N-methyl-D-glucamine (NMG) to pH 6.8 and the desired concentration of CaCl$_2$). Because the NMG$^+$/K$^+$ buffer contained Ca^{2+} in the micromolar range due to impurities of the reagents, measurements at low Ca^{2+} concentrations were carried out in a KP$_i$ buffer (3 mM K$_2$HPO$_4$, 200 μM BAPTA, adjusted with HCl to pH 6.8; final Cl$^-$ concentration was near 2 mM), which was prepared from "suprapur" reagents (Merck, Darmstadt). Ca^{2+} was added as CaCl$_2$. The total Ca^{2+} concentration required for a defined concentration of free Ca^{2+} was calculated according to the method of Tsien (1980) using the program Max Chelator v6.63. K$^+$, H$^+$, and P$_i$ concentration in the medium were taken into account. Because BAPTA is a hygroscopic substance, the concentration of the stock solution was spectroscopically determined by titration with Ca^{2+} (Tsien, 1980). All Ca^{2+} concentrations mentioned below are concentrations of free Ca^{2+}. The Ca^{2+} dependence of the photoreceptor current was determined as follows. For Ca^{2+} concentration changes between 10^{-8} and 10^{-4} M, cells were photoselected in KP$_i$ buffer containing 1 μM Ca^{2+}. For measurements between 10^{-5} and 10^{-2} M Ca^{2+}, cells were photoselected in NMG$^+$/K$^+$ buffer containing 10^{-4} M Ca^{2+}. The pipette was always filled with the preincubation buffer unless indicated otherwise. Buffer containing the different Ca^{2+} concentrations were applied via a trivalved application pipette. After exchanging the buffer, cells were incubated for at least 2 min before the measurements were started.

Suction pipettes with fairly parallel tips (small cone angle) and final tip diameter in the range of 3–4 μm (i.d.) were pulled in two steps from borosilicate glass capillaries (1.7-mm outer diameter, 0.5-mm walls; Hilgenberg, Malsfeld). Pipettes were broken and heat polished according to

the method of Brown and Flaming (1986) and Hamill et al. (1981). In contrast to earlier experiments, the pipettes had an access resistance of 20 to 50 MΩ because of an optimized pipette geometry. Cells were sucked into the pipette by up to one-half until the resistance reached 60 to 150 MΩ. Under these new experimental conditions, one-third of the total current can be detected under the capacitive mode (for further explanation see Harz et al., 1992). Currents were recorded at constant voltage (0 mV between bath and pipette) using a patch-clamp amplifier (EPC-7; List, Darmstadt) and were filtered with a 3-kHz low-pass Bessel filter. Data were recorded and processed with the help of the TL-1–125 labmaster DMA interface and pClamp 5.5.1 software (both from Axon instruments, Foster City, CA). If not otherwise indicated, the shown current traces are the mean of 10 individual sweeps filtered with a digital gaussian filter to 500 Hz. All measurements were carried out at room temperature (20°C). Further details were described by Harz et al. (1992).

Pipettes for measuring P currents directly at the eyespot were pulled from borosilicate glass capillaries (1.8-mm outer diameter, 0.15-mm walls, Kimax-51; Witz Scientific, Maumee, OH) in two steps and were polished until the tip diameter reached 1.5 μm. The cone angle was about 30°. The pipettes were filled and currents were measured in NMG$^+$/K$^+$ buffer containing only 10 μM BAPTA to bind heavy metal ions. The resistance of the pipette was 15–20 MΩ and the seal resistance 120–160 MΩ. A 40$\times$ objective (na = 1.3; Achrostigmat, Zeiss) and a 4$\times$ phototubus were used for identifying the eyespot in infrared light on the screen. Currents were filtered with a 10-kHz low-pass Bessel filter and recorded with a frequency of 100 kHz. The time course of the flash was measured with a photodiode.

The cells were stimulated by a 10-μs flash (IG and G FXQG-949-1; Polytech, Waldbronn). The light was focused on a 1-mm light guide, which was placed at the image plane of an imaging grating (Jobin-Ivon, Grasbrunn) for wavelength selection. The monochromatic light entered the inverted microscope via a second light guide through an epi-illuminescence light path and stimulated the cells through the objective. The flash intensity was regulated either by graded discharge of a set of capacitors (designed by R. Uhl, Technologietransfer, Gräfelfing) or by neutral glass filters. One hundred percent flash intensity (500 nm) corresponds to 1.4 $\times$ 10^{19} photons m^{-2} in the objective plane.

The orientation of the cells was not optimized for maximum light sensitivity, as described before (Harz et al., 1992). In most experiments the eyespot was located at the side, and its surface was more or less parallel to the direction of light incidence.

Motion analysis

Cells (2 $\times$ 10^4 cells/ml) in KP$_i$ buffer with appropriate concentrations of CaCl$_2$, SrCl$_2$, or BaCl$_2$ were recorded after 15 min of preincubation under a light microscope equipped with a 6.3$\times$ objective using infrared light (RG 780 nm; Schott, Mainz, Germany). Images were stored in a computer with a frequency of 30 or 60 Hz, and the net motion of each cell was calculated using a computerized system from Motion Analysis Corporation (MAC, Santa Rosa, CA). Cells were stimulated with green light of 500 nm (selected filter combination SFK 9, 60 nm half-bandwidth; Schott). For analysis the same user program was employed as described before (Hegemann and Bruck, 1989). The average speed was calculated from 10 recordings with a sum of at least 200 cells.

Model for detection of localized ionic currents under different configurations

Before we present experimental details we would like to remind the reader how localized currents are detected in this unicellular alga when suction electrodes are used (Fig. 1). Inward currents that depolarize the cell induce a compensatory charge movement at the outer surface of the plasmalemma due to the capacitor properties of the membrane. Localized currents, as they are P and F currents, are recorded only when the source region is in the pipette as schematized in Fig. 1 a (negative current signals). The P current is represented as a light-regulated conductance in the equivalent
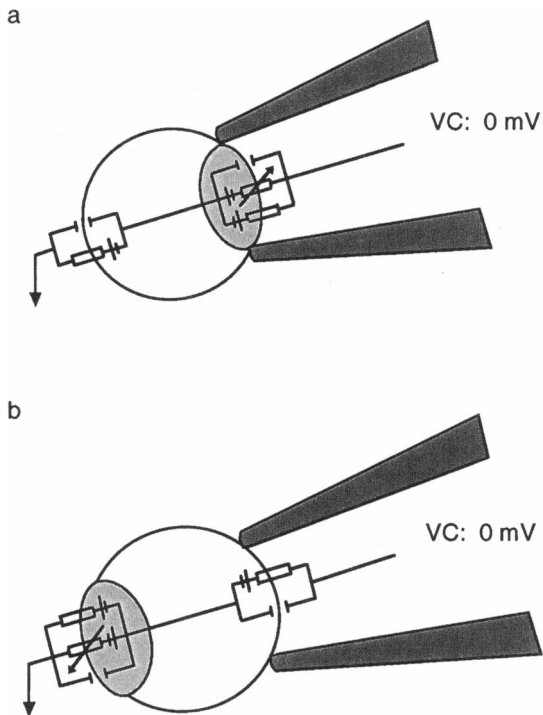
FIGURE 1 Schematic representation of the two measuring configurations with eyespot in (a) or outside (b) the pipette. The major elements of the equivalent circuit are included. During a P current, the membrane conductance increases only in the eyspot region. When the eyespot is in the pipette, the P current is recorded as a real inward current from the pipette into the cell. Consequently, the electromotive force (emf) decreases and decharges the membrane capacitor. Therefore, the photoreceptor current can be detected at any place in the membrane as a capacitive current. Pipette and bath solution are voltage clamped (VC: 0 mV).

circuit diagram of Fig. 1. When the regions conducting the inward currents are outside the pipette (b), only displacement currents can be detected (capacitive mode). The direction of these currents is inverted and thus they are shown as positive current signals. The current signal detectable under these conditions is proportional to the part of the cell surface in the pipette and thus smaller than that under configuration (a). The maximum inward current is observed when the source region with only a small portion of the plasmalemma is in the pipette. Otherwise, an increasing portion of the capacitive current diminishes the recorded inward current (calculated in Harz et al., 1992).

RESULTS

Detection of full-sized P currents

In the early suction experiments the detected P currents were much smaller than the real total P current for two reasons. First, the suction electrodes used had an access resistance on the same order as the seal resistance. Thereby, half of the current was lost via the seal. Second, one-third of the cell was sucked into the pipette, so that one-third of the direct current was counterbalanced by a capacitive current component. It was predicted that the full P current of a single Chlamydomonas gamete must be larger than 40 pA (Harz et al., 1992). Thus, when only the eyespot is sucked into a small patch pipette such that the total resistance is 10

times higher than the access resistance of the pipette, nearly the whole inward current can be detected. Fig. 2 shows such an experiment with a total P current of more than 50 pA. Because the flagella were outside the pipette, only a small portion of the F_F current—proportional to the part of the plasmalemma in the pipette—is detectable. This experiment confirms that the P channels are precisely localized within the eyespot region. Furthermore, this type of experiment allows for the detection of the P current with improved time resolution. As seen in Fig. 2 d, the P current begins with a delay of less than 50 μs after flash, rising to the maximum within 1 ms. There is no early linear phase, as detected in Haematococcus (Sineshchekov et al., 1990). In Chlamydomonas, the rise is not biphasic. Although the late part of the decay is slightly distorted by the small capacitive F_F current in Fig. 2 c, the P current decay was fitted by a single exponential. The P current in Fig. 2 is characterised by $\tau = 0.28$ ms for the rise and $\tau = 2.7$ ms for the decay. Flashes of lower photon exposure cause the τ value to increase inversly proportionally to the peak amplitude (data not shown).
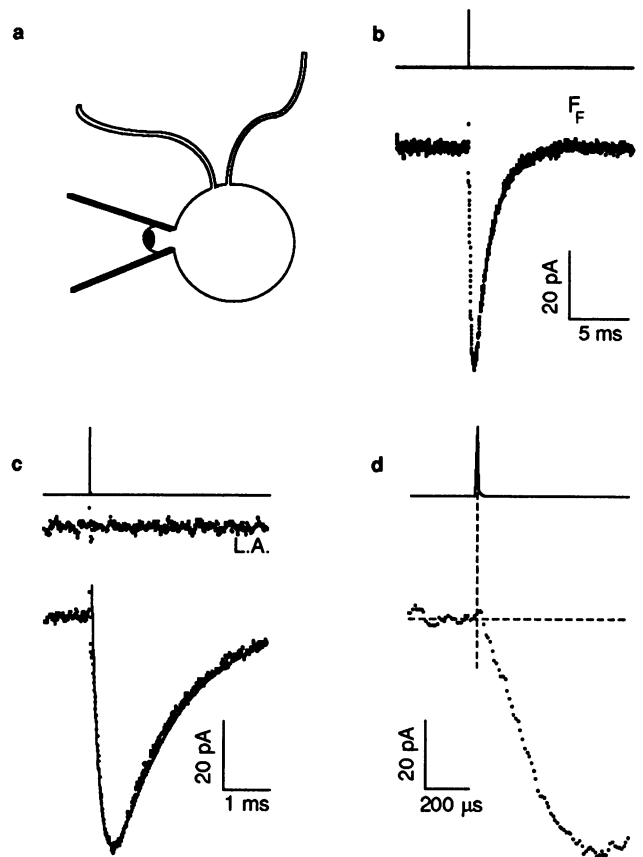

FIGURE 2 Recording of the "full size" P current by applying a patch pipette directly onto the eyespot (a). The P current is plotted at three different time scales. In c the light artefact (L.A.) is shown with the same time resolution as the P current. The rise and the decay are fitted to single exponentials. In d the light artefact has been substracted from the P current. Above all traces, the time course of the flash is plotted as a solid line.

Dependence of photocurrents on divalent ions

From the early measurements on *Haematococcus* (Litvin et al., 1978) and later experiments on *Chlamydomonas* (Harz and Hegemann, 1991; Sineshchekov, 1991a; Harz et al., 1992) it became quite clear that P currents are more or less Ca^{2+} dependent. However, a Ca^{2+} titration over a wide range has never been shown in any alga. Fig. 3 shows a plot of the P current peak amplitude over 6 orders of magnitude of external Ca^{2+}. The Ca^{2+} dependence originally surprised us for several reasons. The rise kinetics and current peak amplitude declined at high Ca^{2+} concentrations. The current maximum was detected at Ca^{2+} concentrations of only 0.3 to 1 μM. A Ca^{2+} contribution was observed down to 100 nM Ca^{2+}. A Ca^{2+}-independent current of less than 30% of the maximum persisted even in the absence of Ca^{2+} in 200 μM BAPTA. Typical photocurrents recorded at three different Ca^{2+} concentrations are presented in Fig. 4. As previously shown, the P current rise is slowed down, the P current maximum is shifted to later times, and the decay is also slowed down when the flash energy is lowered (Harz et al., 1992). This correlation between peak amplitude, time of the maximum, and the decay kinetics is also true for changes of the Ca^{2+} concentration from 300 nM Ca^{2+} to higher values.

To emphasize the ion specificity of the P and F currents, Ca^{2+} was replaced by Sr^{2+}, Ba^{2+}, and Mg^{2+}. In Sr^{2+} the P current remains unchanged, whereas the kinetics of the flagellar currents is significantly altered (Fig. 5 a). In this case, it is difficult to separate F_F from F_S because both currents more or less overlap. Based on individual tracings, we favor the interpretation that F_F remains unchanged,

FIGURE 4 Typical example of photocurrents detected at the three critical Ca^{2+} concentrations closest to the value, where the P current amplitude is at a maximum (0.3 μM).
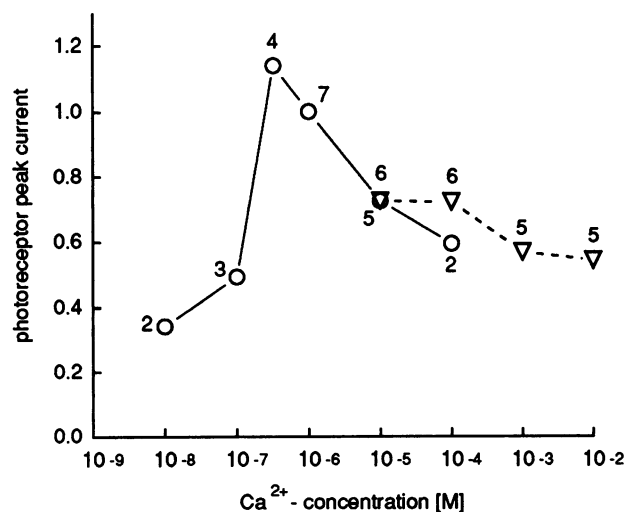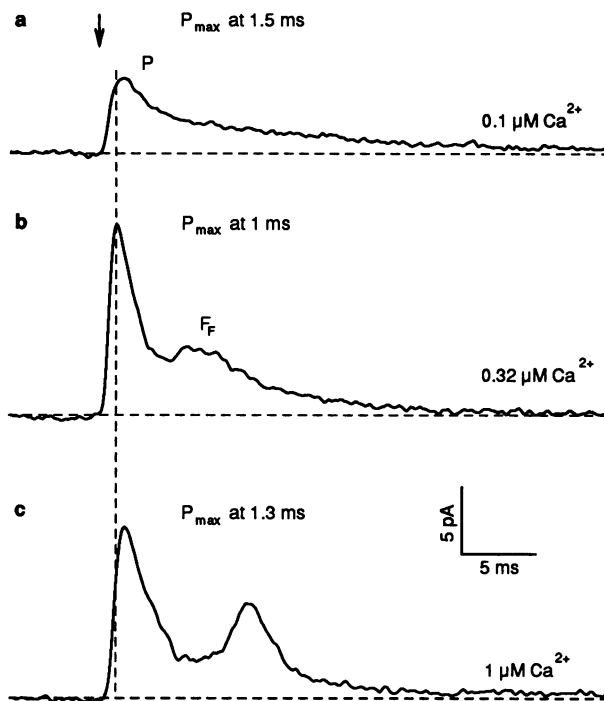

FIGURE 3 The relative photoreceptor peak current amplitude in response to saturating light flashes (100%) is plotted versus the extracellular Ca^{2+} concentration. Concentrations between 10^{-8} and 10^{-4} M Ca^{2+} (*solid line*) were adjusted in KPi buffer, whereas those between 10^{-4} and 10^{-2} M Ca^{2+} (*dashed line*) were prepared in NMG^+/K^+ buffer. Measurements in KPi buffer were normalized to the records at 10^{-6} M, whereas those carried out in NMG^+/K^+ were normalized to the one at 10^{-4} M Ca^{2+}. The number of cells analyzed for each data point is indicated above symbols.

whereas F_S begins with a larger amplitude compared to the control condition but rapidly decays to a low level. Replacement of Ca^{2+} by Ba^{2+} leads to almost unchanged P and F_F current kinetics (b). The P current peak amplitude remains unchanged or only slightly decreases, whereas the F_F current peak is enlarged by 10 to 30%. The F_S current in Ba^{2+} dramatically increases proportionally to the concentration (Fig. 6). At 1 mM Ba^{2+}, the peak amplitude is five- to eightfold larger at maximum compared to control experiments in Ca^{2+}. F_S rises with a delay of about 20 ms after F_F, reaching its maximum 50 ms later. This clear separation in Ba^{2+} justifies the distinction between F_F and F_S. The existence of three different ion channel populations is further supported by a graded sensitivity to Cd^{2+}. F_S shows the highest sensitivity to Cd^{2+}, F_F is less sensitive, and the P current is only influenced very little up to 25 μM Cd^{2+} (Fig. 7). Upon switching from 1 mM Ca^{2+} to 1 mM Mg^{2+}, the P current drops to 10 to 20% of the control and no F currents are observed (Fig. 5 c). The P current is definitively smaller than the residual P current observed in the absence of any divalent ions. However, there are considerable uncertainties. Switching from 100 μM Ca^{2+} to 100 μM Mg^{2+} resulted in a P current that is larger than with no divalent ions. F_F currents detected in 100 μM Mg^{2+} are unusually broad, suggesting unusual on and off kinetics. Because the flagellar membrane is not directly accessible, the signal quality is low, thus precluding a more detailed kinetic analysis. In principle, both P and F channels have a small conductance for Mg^{2+}, but when the external Mg^{2+} con-
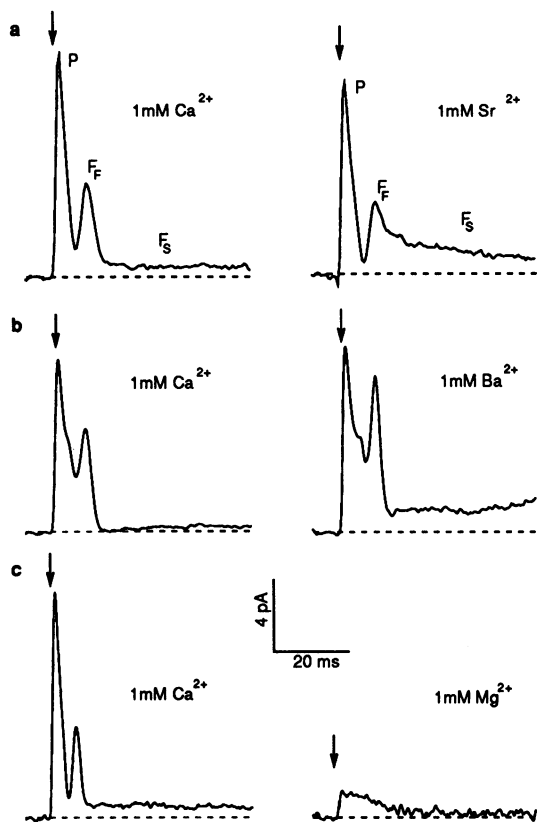
FIGURE 5 The two transient photocurrents recorded at 1 mM Ca^{2+} or Sr^{2+} (a), 1 mM Ca^{2+} or Ba^{2+} (b), or 1 mM Ca^{2+} or Mg^{2+} (c).

FIGURE 6 Photocurrents recorded at 100 μM Ca^{2+} (a), 100 μM Ba^{2+} (b), and 1 mM Ba^{2+} (c).

centration is high (1 mM), the P channel is blocked or inactivated. The inhibitory effect of Mg^{2+} was further demonstrated by adding 1 mM Mg^{2+} to 100 μM Ca^{2+}. Here, P currents were reduced by 70% and F currents completely disappeared. For all tested divalent ions, the same P current integral was needed to trigger flagellar currents. This supports the hypothesis that flagellar currents are voltage-activated events.

It should be mentioned that some cells (one is shown in Fig. 5 b) produce a shoulder within the P current. Because the sign of this component as the P current itself inverts when the eyespot in the pipette, the channels causing the shoulder are clearly in or at least very close to the eyespot.

Motion analysis

From the analysis of how different divalent ions influence the photocurrents it is not immediately clear how these ions affect the photobehavior of the cells. Therefore, in parallel to the electrical measurements photomovement responses were tested. For this purpose 20 to 40 cells were recorded at one time under the microscope. The movement was analyzed with a motion analysis system. The two-dimensional projection of the swimming path together with time coordinates were stored in the computer, and the swimming speed and direction changes were calculated (Hegemann
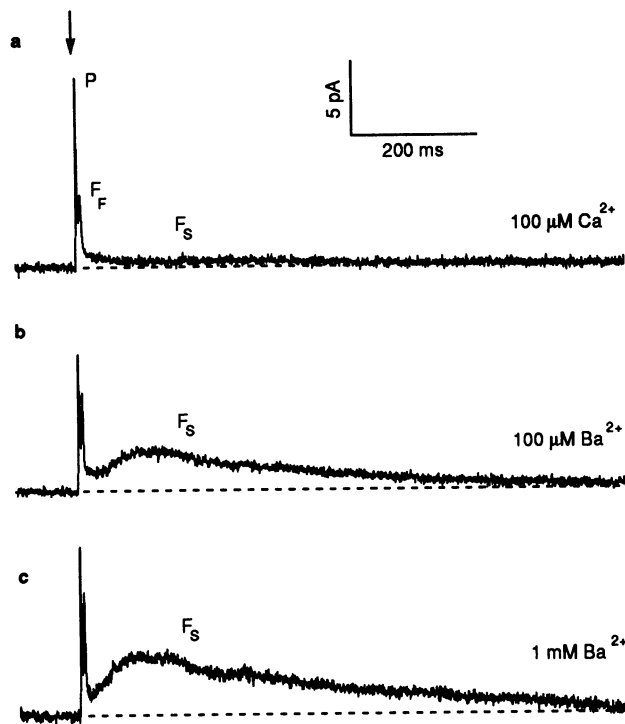
and Bruck, 1989). Upon light stimulation, cells showed a clear stop response with a duration of 600 ms (Fig. 8 a). The swimming paths from these cells clearly showed the slow backward swimming phase. As argued by Harz et al. (1992), F_F initiates the switch from foreward to slow backward swimming, whereas F_S keeps the cell in the backward swimming mode for a total of 600 ms at 100 μM Ca^{2+} or 150 ms at 300 nM Ca^{2+} (Hegemann and Bruck, 1989).

When Ca^{2+} was substituted by Sr^{2+}, the "resting" swimming speed of the cells declined from 100 to 85 μm/s and the duration of the stop response was extended to about 800 to 1100 ms (Fig. 8 b). This is consistent with the enlarged F_S current and a retarded Sr^{2+} removal from the flagellar. With respect to binding to the flagellar structure, Sr^{2+} can substitute Ca^{2+} and induce backward swimming. In a brief abstract, Bean et al. (1982) reported prolonged backward swimming of Chlamydomonas cells in light at 1 mM Sr^{2+}.

When Ca^{2+} is replaced by Ba^{2+}, cells show normal flash-induced speed reduction, but the full swimming speed only recovers very slowly after many seconds (Fig. 8 c). The cells seem to stop and simply remain swimming backward for a longer time. However, a more accurate analysis revealed that cells show an extensive spiraling after a stop response with brief backward swimming (Fig. 9). This lasts 2 to 8 s, depending on the individual cell. The duration of the Ba^{2+} spiraling shows strong variability in a population. Extended spiraling has been observed in 1 mM Ca^{2+} only upon stimulation with long light pulses or step-up stimuli, but it never occurred after a flash. At least in individual cells
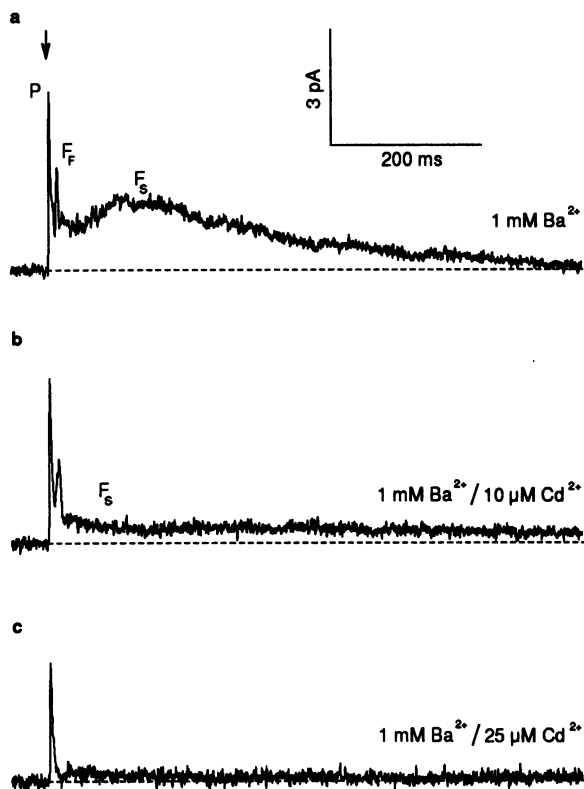
FIGURE 7   Photocurrents recorded at 1 mM Ba^{2+} (a), 1 mM Ba^{2+} and 10 μM Cd^{2+} (b), and 1 mM Ba^{2+} and 25 μM Cd^{2+} (c).

the F_S current is proportional to the duration of the stop response, although under all ionic conditions the duration of the behavioral response extends the duration of F_S. The time of spiraling seems to depend on how fast the cell can extrude or sequester the divalent ions.

DISCUSSION

Characterization and classification of the ion channels on the basis of suction measurements is not an easy task. However, P, F_F, and F_S currents of *Chlamydomonas* have defined characteristics, which may allow a classification as shown in Table 1. The activation of the P channel by a light flash via rhodopsin takes place within 50 μs. In other systems only channels with intrinsic hormone, stretch, or voltage sensors are activated during this time range. This supports the earlier hypothesis stating that in *Chlamydomonas* the rhodopsin and the P channel are closely connected or form one functional unit, and that biochemistry is not involved at this stage of the signal transduction chain. The signal is not amplified on the way between rhodopsin and P channel (Harz et al., 1992, and references therein). Signaling is one or two orders of magnitude faster than the time needed for activating or inactivating ion channels in invertebrate or vertebrate photoreceptors. A rhodopsin, which directly activates a channel, has not been found in any other system so far. But, based on the sequence information, it is
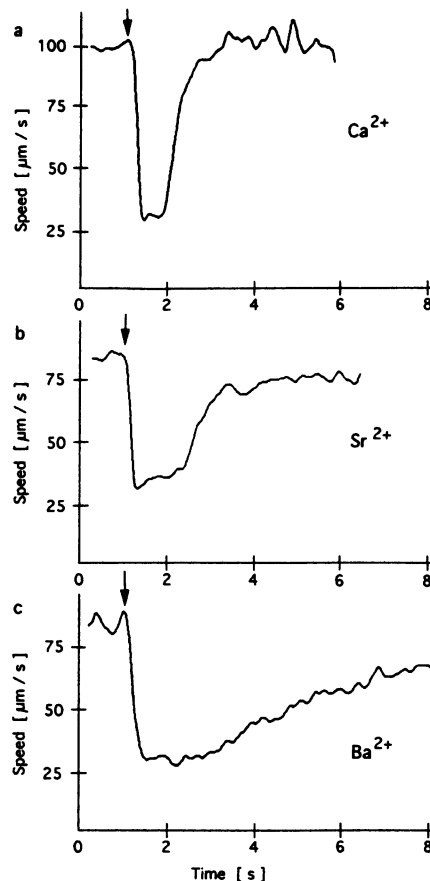

FIGURE 8   Behavioral light responses in presence of 100 μM Ca^{2+} (a), 100 μM Sr^{2+} (b), or 100 μM Ba^{2+} (c). Cells were stimulated with 50-ms light flashes (1.2 × 10^{18} photons m^{-2}). The swimming speed, an average of between 289 and 321 cells, is plotted versus time.

not unlikely that this rhodopsin directly participates in a multimeric ion channel complex (Deininger et al., 1995). The eyespot overlaying part of the plasmelemma contains a high density of intramembrane particles (Melkonian and Robenek, 1984), which might be multimeric ion channel complexes.

Sineshchekov argued that the fast component visible in his experiments represents a charge movement within the photoreceptor molecules (Sineshchekov et al., 1990). In contrast, we have calculated that a charge movement of one charge per rhodopsin is not detectable when there are 10,000 rhodopsin molecules in one cell (strain CW2; Harz et al., 1992). That charge movement is invisible is now supported by the monophasic rise of the P current. However, the finding that chlamyopsin contains 36 Lys brings the charge movement back into the discussion. It will be continued in the accompanying paper.

The photoreceptor (P) channel is activated at a resting potential, which is almost certainly quite negative. Originally on the basis of light titration experiments, where increasing P current peak amplitudes were correlated with a faster decay, it has been suggested that P current inactivation is a voltage-dependent process (Harz et al., 1992). The
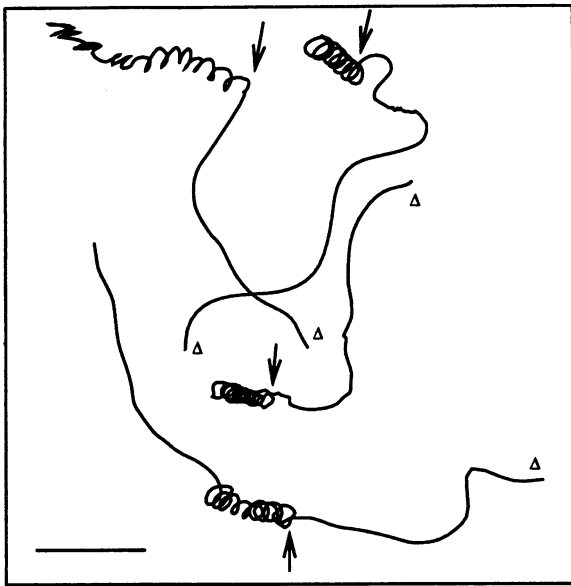
FIGURE 9   Projection traces of free swimming cells between 2 s before and 8 s after stimulation with a 50-ms flash in the presence of 100 μM Ba^{2+}. The start of each trace is indicated by an open triangle. The position of the cells, at which the flash was applied, is indicated by an arrow. Bar = 80 μm.

insensitivity of the P current inactivation to replacement of Ca^{2+} for Sr^{2+} or Ba^{2+} argues against the contribution of divalent ions. One should keep in mind, however, that in addition to channel inactivation, declining driving forces, as they are the membrane voltage itself, and the Ca^{2+}-gradient also contribute to the current decay.

On one hand saturation of the P current at Ca^{2+} concentrations below 1 μM suggests an extremely tight binding of Ca^{2+} to the channel and, on the other hand it indicates an unusually small unitary conductance. A high binding constant for Ca^{2+} makes sense for an organism that has to cope with very low extracellular ion concentrations. Because tight binding of Ca^{2+} decreases the throughput of the channel (Yellen, 1993), it can explain the low saturation level and a low conductance of the P current equally well. It should be kept in mind that this situation totally differs from that of animal cells, which are exposed to high and controlled ionic conditions. For those cells tight Ca^{2+} binding is unneccessary.

As a general theme in biology, ligand-gated channels create an initial depolarization that enables the cell to fire short action potentials. In turn, these action potentials open high-voltage-activated (HVA) Ca^{2+} channels that keep the cell depolarized for up to some hundred milliseconds. In Chlamydomonas, the action-potential-like activity is represented by the fast and transient F_F currents, which appear as all-or-none events. Inhibitor studies on Haematococcus and Chlamydomonas, together with the higher F_F current amplitude in Ba^{2+} and the low amplitude in absence of Ca^{2+} at low pH, are cumulative indicators that the inward F_F current under physiological conditions is mainly carried by

TABLE 1   Photocurrents in Chlamydomonas

Name	P current	F_F current	F_S current
Location	Eyespot region	Flagella	Flagella
Activated by	Rhodopsin	Voltage	Voltage
Suggested activation range	Neg. potentials	Neg/pos	Neg/pos
Decay rate	Fast	Fast	Slow
	τ: 2.4–12 ms	τ: 3–4 ms	τ: >100 ms
Rel conductance	$Ba^{2+} = Ca^{2+}$	$Ba^{2+} > Ca^{2+}$	$Ba^{2+} >> Ca^{2+}$.

Ca^{2+}. The unchanged decay rate at various flash energies and different Ca^{2+} or Ba^{2+} concentrations reveals that F_F current inactivation is a spontaneous process.

Because Ca^{2+} is the physiologically most important ion for behavioral responses, it would be interesting to know more about the Ca^{2+} concentration changes within the flagella during the time period of the photocurrents. Several conclusions about the conjuction between the Ca^{2+} concentration and the flagellar beating have been drawn from studies using isolated demembranated flagellar apparatuses or single isolated flagellar axonemes. At Ca^{2+} concentrations of less than 10^{-5} M, reactivated axonemes beat with a waveform similar to that of intact flagella. Yet at 10^{-4} M Ca^{2+}, they switch to a waveform which is similar to that of slow backward-swimming cells during a stop response (Bessen et al., 1980). In Triton-extracted cells (cell models), the ciliary reversal occurs at lower Ca^{2+} concentrations of more than 10^{-6} M. At 10^{-3} M Ca^{2+}, motion was totally inhibited or flagella were detached from the cell body (Kamiya and Witman, 1984; Witman, 1994). In those experiments exclusively equilibrium concentrations for beating changes were determined.

In contrast to the studies with cell models or isolated flagella, electrical measurements of this study detect the amount of Ca^{2+} that enters the flagella and appears as free plus protein-bound Ca^{2+}. F_F currents with measured current integrals of between 23 and 80 fQ reflect a total Ca^{2+} influx of 70 and 240 fQ, because only 30% of the current is detected, as discussed above. These currents cause the Ca^{2+} concentration within the flagella to increase by 3 $\times$ 10^{-4} to 1 $\times$ 10^{-3} M, assuming a flagellar diameter of 250 nm and a total flagellar volume of 5 $\times$ 10^{-16} liter. During F_S, the Ca^{2+} concentration should rise even further. Slow Ba^{2+} currents with integrals of up to 3 pQ increases the concentration of divalent ions to more than 10 mM. Because this concentration exceeds the extracellular Ba^{2+} concentration, the Ba^{2+} must be bound to intraflagellar proteins or the membrane potential must be still quite negative at this stage. Moreover, the concentrations calculated for Ca^{2+} by far exceed those determined for backward swimming of permeabilized Chlamydomonas cell models or isolated flagellar apparatuses (Bessen et al., 1980; Kamiya and Witman, 1984). When Ca^{2+} is tightly bound to flagellar proteins, the concentration of free Ca^{2+} is kept at fairly low levels and the Ca^{2+} and Ba^{2+} gradients are maintained. From the Ca^{2+}

pool apparently only a very small amount is free Ca^{2+}. So, we assume that we primarily measure the Ca^{2+} binding places of the flagella that become occupied during a switch from foreward to slow backward swimming.

REFERENCES

Bean, B., R. Savitsky, and B. Grossinger. 1982. Strontium ion (Sr^{2+}) induces backward swimming of *Chlamydomonas*. *J. Protozool.* 29:63a.

Beck, C., and R. Uhl. 1994. On the localisation of voltage sensitive calcium channels in the flagella of *Chlamydomonas*. *J. Cell Biol.* 125: 1119–1125.

Beckmann, M., and P. Hegemann. 1991. In vitro identification of rhodopsin in the green alga *Chlamydomonas*. *Biochemistry.* 30:3692–3697.

Bessen, M., R. B. Fay, and G. B. Witman. 1980. Calcium control of waveform in isolated flagellar axonemes of *Chlamydomonas*. *J. Cell Biol.* 86:446–455.

Boskov, J. S., and M. E. Feinleib. 1979. Phototactic responses of *Chlamydomonas* to flashes of light. II. Response of individual cells. *Photochem. Photobiol.* 30:499–505.

Brown, K. T., and D. G. Flaming. 1986. Advanced micropipette techniques for cell physiology. *In* IBRO Handbook series: Methods in Neurosciences, Vol. 9. Chichester, John Wiley and Sons. 139–141.

Deininger, W., P. Kröger, U. Hegemann, F. Lottspeich, and P. Hegemann. 1995. Chlamyrhodopsin represents a new type of sensory photoreceptor. *EMBO J.* In press.

Foster, K. W., J. Saranak, N. Patel, G. Zarilli, M. Okabe, T. Kline, and K. Nakanishi. 1984. A rhodopsin is the functional photoreceptor for phototaxis in the unicellular eukaryote *Chlamydomonas*. *Nature.* 311: 756–759.

Hamill, O. P., A. Marty, E. Neher, B. Sakmann, and F. J. Sigworth. 1981. Improved patch clamp techniques for high resolution current recording from cells and cell free membrane patches. *Pflügers Arch. Eur. J. Physiol.* 391:85–100.

Harz, H., and P. Hegemann. 1991. Rhodopsin regulated calcium currents in *Chlamydomonas*. *Nature.* 351:489–491.

Harz, H., C. Nonnengässer, and P. Hegemann. 1992. The photoreceptor current of the green alga *Chlamydomonas*. *Phil. Trans. R. Soc. Lond. B* 338:39–52.

Hegemann, P., and B. Bruck. 1989. Light-induced stop response in *Chlamydomonas reinhardtii*. Occurrence and adaptation phenomena. *Cell Motil.* 14:501–515.

Hegemann, P., W. Gärtner, and R. Uhl. 1991. All-trans retinal constitutes the fuctional chromophore in *Chlamydomonas* rhodopsin. *Biophys. J.* 60:1477–1489.

Hegemann, P., and W. Marwan. 1988. Single photons are sufficient to trigger movement responses in *Chlamydomonas reinhardtii*. *Photochem. Photobiol.* 48:99–106.

Kamiya, R., and G. B. Witman. 1984. Submicromolar levels of calcium control the balance of beating between the two flagella in demembranated cell models of *Chlamydomonas*. *J. Cell Biol.* 98:97–107.

Lawson, M. A., D. N. Zacks, F. Derguini, K. Nakanishi, and J. L. Spudich. 1991. Retinal analog restoration of photophobic responses in a blind *Chlamydomonas reinhardtii* mutant. *Biophys. J.* 60:1490–1498.

Litvin, F. F., O. A. Sineshchekov, and V. A. Sineshchekov. 1978. Photoreceptor electric potential in the phototaxis of the alga *Haematococcus pluvialis*. *Nature.* 271:476–478.

Melkonian, M., and H. Robeneck. 1984. The eyespot apparatus of flagellated green algae: a critical review. *Progr. Phycol. Res..* 3:193–286.

Nichols, K. M., and R. Rikmanspoel. 1978. Control of flagellar motion in *Chlamydomonas* and *Euglena* by mechanical microinjection of Mg^{2+} and Ca^{2+} and by electric current injection. *J. Cell Sci.* 29:233–247.

Nonnengasser, C., E.-M. Holland, H. Harz, and P. Hegemann. 1996. The nature of rhodopsin-triggered photocurrents in *Chlamydomonas*. II. Influence of monovalent ions. *Biophys. J.* 70:000–000.

Schmidt, J. A., and R. Eckert. 1976. Calcium couples flagellar reversal to photostimulation in *Chlamydomonas reinhardtii*. *Nature.* 262:713–715.

Sineshchekov, O. A. 1991a. Electrophysiology of photomovements in flagellated algae. *In* Biophysics of Photoreceptors and Photomovements in Microorganisms. F. Lenci, F. Ghetti, G. Colombetti, D.-P. Häder, and P. S. Song, editors. Plenum Press, New York. 191–202.

Sineshchekov, O. A. 1991b. Photoreception in unicellular flagellates: bioelectric phenomena in phototaxis. *In* Light in Biology and Medicine, Vol. 2. R. H. Douglas, editor. Plenum Press, New York. 523–532.

Sineshchekov, O. A., F. F. Litvin, and L. Keszethely. 1990. Two components of the photoreceptor potential in phototaxis of the flagellated green alga *Haematococcus pluvialis*. *Biophys. J.* 57:33–39.

Sullivan, J. M., and K. W. Foster. 1987. Light dependent ion channel activity in *Chlamydomonas*. *Biophys. J.* 51:274a.

Takahashi, T., K. Yoshihara, M. Watanabe, M. Kubota, R. Johnson, F. Derguini, and K. Nakanishi. 1991. Photoisomerisation of retinal at 13-ene is important for phototaxis of *Chlamydomonas reinhardtii*: simultaneous measurements of phototactic and photophobic responses. *Biochem. Biophys. Res. Commun.* 178:1273–1279.

Tsien, R. Y. 1980. New calcium indicators and buffers with high selectivity against magnesium and protons: design, synthesis, and properties of prototype structures. *Biochemistry.* 19:2396–2404.

Uhl, R., and P. Hegemann. 1990. Probing visual transduction in a plant cell. Optical recording of rhodopsin-induced structural changes from *Chlamydomonas reinhardtii*. *Biophys. J.* 58:1295–1302.

Witman, G. B. 1994. *Chlamydomonas* phototaxis. *Trends Cell Biol.* 3:403–408.

Yan, B., K. Nakanishi, and J. L. Spudich. 1991 Mechanism of activation of sensory rhodopsin. I. Evidence for a steric trigger. *Proc. Natl. Acad. Sci USA.* 88:9412–9416.

Yellen, G. 1993 Calcium channels: structure and selectivity. *Nature.* 366: 109–110.

Zacks, D. N., F. Derguini, K. Nakanishi, and J. L. Spudich. 1993. Comparative study of phototactic and photophobic receptor chromophore properties in *Chlamydomonas reinhardtii*. *Biophys. J.* 65:508–518.